Bio-Based Chemicals

Yuan, Qingqing; Hiemstra, Kevin; Meinds, Tim G.; Chaabane, Ibrahim; Tang, Zhenchen; Rohrbach, Leon; Vrijburg, Wilbert; Verhoeven, Tiny; Hensen, Emiel J. M.; van der Veer, Siebe

Published in:
ACS Sustainable Chemistry & Engineering

DOI:
10.1021/acssuschemeng.8b03821

Publication date:
2019

ACS Sustainable Chemistry & Engineering

Research Article

Cite This: ACS Sustainable Chem. Eng. 2019, 7, 4647−4656

pubs.acs.org/journal/ascecg

Bio-Based Chemicals: Selective Aerobic Oxidation of Tetrahydrofuran-2,5-dimethanol to Tetrahydrofuran-2,5-dicarboxylic Acid Using Hydrotalcite-Supported Gold Catalysts

Qingqing Yuan,[†] Kevin Hiemstra,[†] Tim G. Meinds,[†] Ibrahim Chaabane,[†] Zhenchen Tang,[†] Leon Rohrbach,[†] Wilbert Vrijburg,[‡] Tiny Verhoeven,[‡] Emiel J. M. Hensen,[‡] Siebe van der Veer,[§] Paolo P. Pescarmona,[†] Hero J. Heeres,[†] and Peter J. Deuss*[,†]

[†]Department of Chemical Engineering (ENTEG), University of Groningen, Nijenborgh 4, 9747 AG Groningen, The Netherlands

[‡]Laboratory of Inorganic Materials Chemistry, Schuit Institute of Catalysis, Department of Chemical Engineering and Chemistry, Eindhoven University of Technology, 5612 AZ Eindhoven, The Netherlands

[§]Kisuma Chemicals B.V, Billitonweg 7, 9641 KZ Veendam, The Netherlands

Supporting Information

ABSTRACT: A new, sustainable catalytic route for the synthesis of tetrahydrofuran-2,5-dicarboxylic acid (THFDCA), a compound with potential application in polymer industry, is presented starting from the bio-based platform chemical 5-(hydroxymethyl)furfural (HMF). This conversion was successfully achieved via oxidation of tetrahydrofuran-2,5-dimethanol (THFDM) over hydrotalcite (HT)-supported gold nanoparticle catalysts (~2 wt %) in water. THFDM was readily obtained with high yield (>99%) from HMF at a demonstrated 20 g scale by catalytic hydrogenation. The highest yield of THFDCA (91%) was achieved after 7 h at 110 °C under 30 bar air pressure and without addition of a homogeneous base. Additionally, Au−Cu bimetallic catalysts supported on HT were prepared and showed enhanced activity at lower temperature compared to the monometallic gold catalysts. In addition to THFDCA, the intermediate oxidation product with one alcohol and one carboxylic acid group (5-hydroxymethyl tetrahydrofuran-2-carboxylic acid, THFCA) was identified and isolated from the reactions. Further investigations indicated that the gold nanoparticle size and basicity of HT supports significantly influence the performance of the catalyst and that sintering of gold nanoparticles was the main pathway for catalyst deactivation. Operation in a continuous setup using one of the Au−Cu catalysts revealed that product adsorption and deposition also contributes to a decrease in catalyst performance.

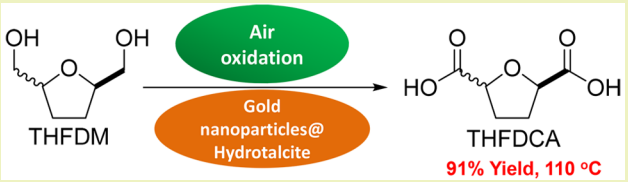

KEYWORDS: *Gold catalysts, Tetrahydrofuran-2,5-dimethanol, Hydrotalcite, Renewable chemicals, Oxidation catalysis*

INTRODUCTION

The drive toward a sustainable chemical industry that relies on renewable resources has led to intensified research in the conversion of biomass to fuels and chemicals. A number of interesting target molecules have been identified (platform chemicals) based on criteria such as yields and potential for chemical diversification.[1] 5-Hydroxymethylfurfural (HMF) is among the most attractive platform chemicals with significant market potential.[2] It can be readily produced from C6 sugars (e.g., D-glucose and D-fructose),[3] which can be derived from second generation lignocellulosic feedstocks. HMF can also be the starting material toward many useful chemicals, such as 2,5-furan dicarboxylic acid (FDCA),[4] tetrahydrofuran-2,5-dimethanol (THFDM),[5] tetrahydrofuran-2,5-dicarboxylic acid (THFDCA),[6] 1,6-hexanediol,[7] caprolactone, and caprolactam,[8] as well as 1,2,4-benzenetriol (BTO) and cyclohexanone[9] (Scheme 1), many of which can find application as polymer building blocks. For example, FDCA has been used to replace terephthalic acid in poly(ethylene terephthalate) (PET) resulting in poly(ethylene furanoate) (PEF), which has several superior properties compared to PET.[10] The utilization of a saturated furan compound such as THFDCA for new polymeric materials[11] is also of great interest as a nonaromatic alternative to FDCA. THFDCA is also considered as an appealing building block to produce adipic acid[12−14] esters,[15] or prodrugs.[16]

A previously reported strategy for the synthesis of THFDCA from HMF involves the oxidation of HMF to FDCA followed by reduction of the furan ring (route 1, Scheme 1). The oxidation of HMF to FDCA has been extensively studied in the past decade and is well established.[4,17−20] Also, the conversion to THFDCA from FDCA has been described using several catalysts.[6,12,13]

The highest yield of THFDCA (88%) was achieved using a Pd/SiO_2 catalyst in acetic acid. However, the use of acetic acid is not ideal due to its corrosiveness and difficulties regarding

Received: August 3, 2018
Revised: January 21, 2019
Published: January 30, 2019

DOI: 10.1021/acssuschemeng.8b03821
ACS Sustainable Chem. Eng. 2019, 7, 4647−4656

Scheme 1. Selection of HMF Derived Chemicals That Have Potential As Renewable Monomers for Polymeric Products[a]

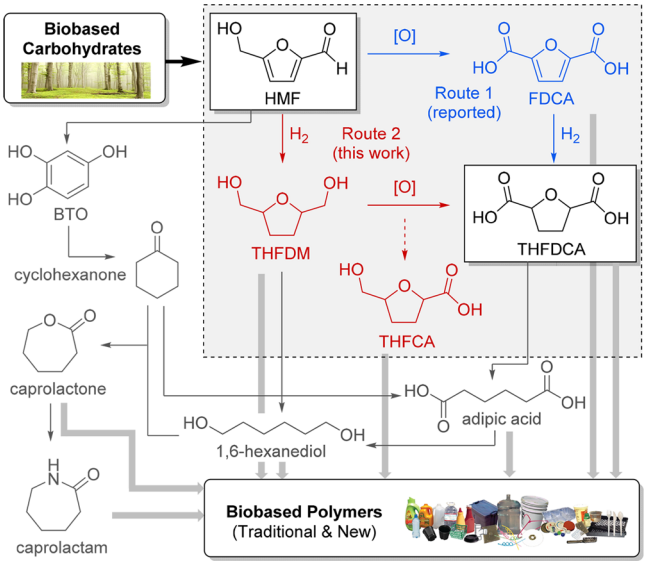

[a]Highlighted are the two main strategies (routes 1 and 2) to obtain THFDCA, the target product in this work.

downstream processing. Additionally, during the reduction of FDCA, byproducts such as 5-formylfuran-2-carboxylic acid and 2,5-diformylfuran (DFF) are formed. Such byproducts can be avoided by taking an alternative route where HMF is reduced to THFDM, which is subsequently oxidized to THFDCA (route 2, Scheme 1). THFDM can be obtained in high yield (>99%) by reduction of HMF using a Pd/Al_2O_3 catalyst under mild conditions.[5] To obtain THFDCA from THFDM, an effective catalytic system for the oxidation step is still required. Haworth et al. tried to oxidize THFDM to THFDCA by using a homogeneous chromic anhydride catalyst, but only degradation products were formed.[13]

Here, we report for the first time the successful oxidation of THFDM to THFDCA with excellent yield. In our system, no side products such as esters were formed and the conversion of both alcohols of THFDM to carboxylic acids was achieved without the detection of significant amounts of aldehydes. Additionally, this oxidation was performed using heterogeneous catalysts that operate in water as solvent, use air as oxidant, and do not require the addition of a homogeneous base. Moreover, this sustainable catalytic route also offers access to 5-(hydroxymethyl) tetrahydrofuran-2-carboxylic acid (THFCA), which is another interesting HMF-derived product (Scheme 1). The first catalytic system that we studied consisted of gold nanoparticles supported on hydrotalcite (HT). Gold nanoparticles have proven to be very selective for the oxidation of primary alcohols to carboxylic acids, but a common major drawback is the need for homogeneous bases such as NaOH or Na_2CO_3 to help formation of the required alkoxide species.[21,22] As an alternative, solid bases as catalyst supports were explored.[23,24] In addition, the gold has been used as the active metal in which it was shown that the particle size has a strong effect on the activity in alcohol oxidations,[25−27] especially for Au/HT catalysts. Fang et al.[26] showed that for Au/HT catalysts with the same metal loading the turnover frequency (TOF) for benzyl alcohol oxidation increased as particle size decreased.

Polar solvents tend to accelerate the oxidation reaction of primary alcohols.[22] Therefore, water is an excellent choice for the deep oxidation to carboxylic acid.[28,29] Zope et al.[28] reported that the catalytic decomposition of a peroxide intermediate from molecular oxygen forms hydroxide ions, which facilitate the oxidation of alcohols in aqueous media. Later, the same group used labeled $^{18}O_2$ and $H_2{}^{18}O$ to prove that water rather than O_2 was the source of oxygen atoms in the oxidation of HMF to FDCA.[29] Moreover, water as solvent is environmentally benign, safe, cheap, and easy to handle. Therefore, it is an ideal medium for the sustainable conversion of biomass-derived feedstocks such as those reported in this work.

EXPERIMENTAL SECTION

Materials. Hydrotalcites (HT) were kindly provided from Kisuma Chemicals. THFDM was obtained with a high yield (>95%) by scale-up reduction of HMF (20 g) using a commercial Pd/Al_2O_3 catalyst as described in the literature[5] and further purified by distillation (>99% purity according to ^1H NMR). Cis/trans ratio was determined to be 9:1 from the ^1H NMR. Milli-Q water was used, $HAuCl_4$ was obtained from Strem, and other chemicals were purchased from Sigma-Aldrich. All chemicals were used as received.

Catalyst Preparation. *Synthesis of Au/HT Catalysts.* Au/HT samples (2 wt %) were prepared by a deposition−precipitation method. Typically, 8 mL of $HAuCl_4{\cdot}H_2O$ aqueous solution (10 mg Au/mL), 9.94 g of urea (urea/Au = 400:1 molar ratio), 4 g of hydrotalcite, and 100 mL of H_2O were mixed in a 250 mL round-bottom flask, covered with aluminum foil to prevent interference from light. The obtained orange color suspension was placed in an oil bath at 80 °C, while stirring at 650 rpm for 6 h, after which it was stirred overnight at room temperature. Subsequently, the suspension was filtered and washed with water (4 L), the obtained yellow substance was dried overnight at 85 °C. The product was ground and subsequently calcined under a flow of air at 200 °C using a temperature ramp of 3.33 °C/min from room temperature for 5 h. After calcination, a purplish powder (>85% yield) was obtained.

Synthesis of Au−Cu/HT Bimetallic Catalysts. Au−Cu/HT bimetallic catalysts were prepared by the sequential deposition−precipitation method as described in literature.[30] Typically, for a 3 wt % Au−Cu/HT catalyst, copper was first deposited on the hydrotalcite: 99.7 mg of $Cu(NO_3)_2$, 10.06 g of urea (urea/Cu = 400:1 molar ratio), 4 g of hydrotalcite, and 100 mL of H_2O were mixed in a 250 mL round-bottom flask, covered with aluminum foil to prevent interference from light. The obtained blue color suspension was placed in an oil bath at 80 °C, while stirring at 650 rpm for 6 h, after which it was stirred overnight at room temperature. Subsequently, the suspension was filtered and washed with H_2O (4 L). The obtained blueish substance was dried overnight at 85 °C. Subsequently, gold was deposited on the uncalcined Cu/HT by the same procedure. The resulting green cake was ground into a fine powder and split into two fractions. One of the fractions was calcined under a flow of air at 200 °C with a temperature ramp of 3.33 °C/min from room temperature for 5 h (AuCu-A/HT), while the other batch was reduced under H_2 instead of an air flow (AuCu-B/HT).

The catalyst preparation was successfully scaled-up to 20 g of Au/HT-1, AuCu-A/HT, and AuCu-B/HT. The only deviation from the above procedures was that in this case the catalysts were washed with water until the pH value of filtered water equaled 7. The catalytic performance results from different catalyst batches are collected in Table S3.

Catalyst Characterization. Inductively coupled plasma-optical emission spectrometry (ICP-OES) was used to determine the metal loading on the support (Tables S1 and S2). The samples were prepared by microwave treatment in aqua regia. The analysis was performed on a PerkinElmer Optima 7000 DV apparatus using a solid-state CCD array detector. Argon was used as purge gas and yttrium (10 ppm) and scandium (10 ppm) as internal standards.

DOI: 10.1021/acssuschemeng.8b03821
ACS Sustainable Chem. Eng. 2019, 7, 4647−4656

Table 1. Experimental Results for the Oxidation of THFDM Using Au/HT Catalysts[a]

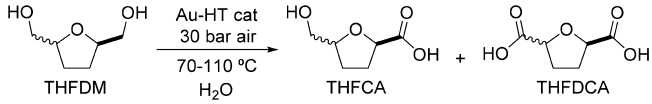

entry	catalyst	time (h)	temp (°C)	conv. (%)	yield (%)	
					THFCA	THFDCA
1	HT-1[b]	5	110	8	0	0
2	Au/HT-1	7	110	97	17	80
3	Au/HT-2	7	110	89	36	49
4	Au/HT-3	7	110	98	6	91
5[c]	Au/HT-1	5	90	79 ± 8	43.5 ± 6.5	35.5 ± 10.5
6	Au/HT-2	7	90	18	3	1
7	Au/HT-3	5	90	7	0	0.5
8	Au/HT-1	5	70	2	0	0

[a]Reaction conditions: 30 mL of 0.02 M THFDM in water, THFDM/Au = 40:1 (molar ratio), catalyst amount ca. 0.17 g, 30 bar air pressure, 600 rpm. [b]0.2 g of catalyst. [c]Error values represent standard deviations derived from results obtained from experiments using separately prepared batches of this catalyst (Table S3).

X-ray fluorescence (XRF) is also applied to determine the magnesium and aluminum content of the support (Tables S1 and S2). XRF data were recorded on a PANalytical Axios spectrometer or a Philips PW 2404 spectrometer equipped with a Rh-tube. Samples were prepared by destruction of the material in a flux. The substance (1.8 g) was dissolved in 9 g of lithium borate flux (67% $Li_2B_4O_7$/33% $LiBO_2$) at 1200 °C.

X-ray photoelectron spectroscopy (XPS) measurements were performed on a Thermo Scientific K-Alpha, equipped with a monochromatic small-spot X-ray source and a 180° double focusing hemispherical analyzer with a 128-channel detector. Spectra were obtained using an aluminum anode (Al Kα = 1486.6 eV) operating at 72 W and a spot size of 400 μm. Survey scans and region scans were measured at a constant pass energy of 200 and 50 eV, respectively. The background pressure was below 8.0×10^{-8} mbar. Data analysis was carried out using CasaXPS, and binding energies were charge-corrected using the C 1s = 284.8 eV peak of adventitious carbon as a reference. Experimental error range is ±0.1 eV.

Transmission electron microscopy (TEM) images were measured and obtained using a Tecnai T20 electron microscope (FEI) with a high-angle annular dark-field (HAADF) scanning TEM (STEM) detector operated at 200 kV. The average particle diameter was calculated using eq 1 for at least 50 nanoparticles.

$$d_{avg} = \frac{\sum_1^n d_1^3 + \ldots d_n^3}{\sum_1^n d_1^2 + \ldots d_n^2} \quad (1)$$

Reaction Procedure and Product Analysis. THFDM oxidation reactions at elevated pressure were performed in a stainless-steel autoclave without insert. Typically the catalyst and 30 mL of 0.02 M THFDM aqueous solution (THFDM/Au = 40:1, molar ratio) were added to the metal insert, which was placed under the stirrer. The reactor was closed, sealed, and pressurized to 30 bar air, below the lower explosive limit assuming THFDM as methanol (which is 5% v/v). Temperatures were varied, but typically the reaction would be done at 90 °C for 5 h with a stirring speed of 600 rpm. After the reaction, the reactor was cooled to room temperature and depressurized. The catalyst was separated from the substrate/product mixture with a syringe filter (0.45 μm). The filtered reaction solution was analyzed by HPLC (Agilent Technologies 1200 series, a Bio-Rad Aminex HPX-87H 300 mm × 7.8 mm column, T = 60 °C, with 0.5 mM H_2SO_4 as an eluent (flow rate 0.55 mL/min). 2-Butanone was added to the HPLC sample as internal standard. After reaction, the catalyst was collected and dried at 85 °C overnight for TEM analysis.

An analytically pure sample of THFCA was obtained using the BUCHI Reveleris PREP purification system and a BUCHI C_{18} column (150 mm × 21.2 mm × 10 μm). Fractions were eluted with a gradient of acetonitrile in water (0−100%) at a flow rate of 15 mL/min over 17 min. Detection of chemical compounds was achieved with a UV and ELSD detector. UV detection was set at three different wavelengths: 254, 280, and 560 nm. Based on the UV and ELSD profiles, individual fractions were collected, and the solvent was removed by rotary evaporation. The remaining solids were dissolved in DMSO-d_6 analyzed by NMR yielding a pure fraction that was identified as THFCA.

Recycling of the Catalysts. For recycling studies, the catalyst was separated from the reaction mixture by centrifugation at 3500 rpm for 5 min. The catalyst was then washed thoroughly with *n*-pentane, methanol, and water and dried overnight, and a secondary run was done following the same oxidation procedure at 90 °C. 2-Butanone was added to the HPLC sample as internal standard.

THFDM Oxidation in a Continuous Setup. THFDM oxidation reactions at elevated pressure and 101 °C were performed in a continuous setup (Figure S6). The reactor tube was typically loaded with 0.4 g of catalyst. The catalyst was mixed with silicon carbide before addition to the fixed-bed to ensure a better flow. Before reaction, the flow was tested with 0.5 mL/min water and 100 mL/min air at 30 bar. Stock solutions used for this setup were 0.01 M THFDM with dipropyl sulfone as internal standard. Samples were taken every 4 h automatically by an in-house made sampling robot. The samples were analyzed by HPLC.

RESULTS AND DISCUSSION

Influence of Different HT Supports. We set out to develop a catalytic system for the sustainable oxidation of THFDM to THFDCA. For the reasons mentioned above, we decided to start our study with gold nanoparticles on basic HT supports. The gold catalysts (2 wt %) were prepared using deposition−precipitation (Tables S1 and S2 for Mg/Al ratio and basicity of the support, metal loading, and particle size of the catalysts). Analysis by XRD of the hydrotalcite samples before and after supporting of the metal nanoparticles showed some changes upon metal deposition and calcination (i.e., broadening of the peaks, shift to higher angles of the peak at 11°, decrease in the intensity of the peak at 22°, see Figure S1). Similar changes have been observed in previous work and are likely to be caused by loss of order in the layered structure of hydrotalcite, loss of interlayer water, and ion exchange of carbonate ions with chloride ions originating from the gold precursor (i.e., $HAuCl_4$).[31−35] To investigate the effect of the HT on the catalytic performance for THFDM oxidation in water, three different HT supports were employed (HT-1, HT-2, and HT-3 with Mg/Al molar ratios of 4.1, 2.9, and 1,

DOI: 10.1021/acssuschemeng.8b03821
ACS Sustainable Chem. Eng. 2019, 7, 4647−4656

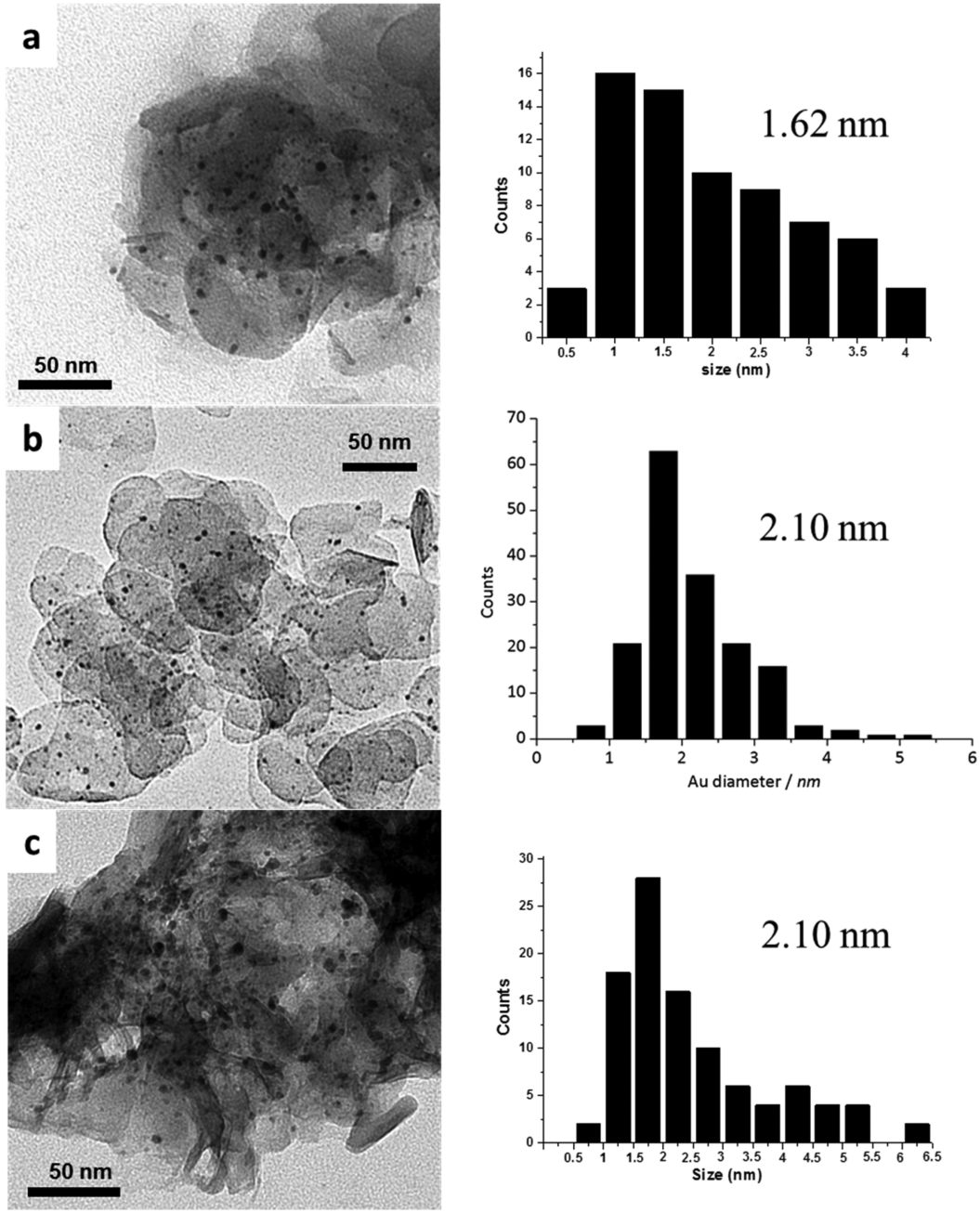

Figure 1. TEM images (left) and particle size distributions (right) of Au/HTs: (a) Au/HT-1; (b) Au/HT-2; (c) Au/HT-3.

respectively). These catalysts were tested for the oxidation of THFDM to THFDCA in batch reactors under 30 bar air pressure at temperatures from 70 to 110 °C (Table 1).

An experiment with only HT loaded in the reactor proved that the support has no oxidation activity for THFDM (Table 1, entry 1). If the reaction was carried out at 110 °C, the conversion of THFDM exceeded 89% for all Au/HT catalysts (Table 1, entries 2−4). The main oxidation products from THFDM were THFCA (vide infra) and THFDCA, with some differences in THFDCA yield. An excellent yield of 91% for THFDCA was obtained using Au/HT-3, demonstrating the potential of these catalysts. In all cases, the cis/trans ratio was determined to be around 9.5:1 by ^{1}H NMR analysis. This was close to the 9:1 ratio determined for THFDM obtained from the reduction of HMF using Pd/Al_2O_3 in ethanol,[5] which was used as substrate for these reactions. To illustrate the merit of this new route to THFDCA, the calculated E-factor of THFCA/THFDCA via THFDM was 0.07 based on these initial results, which is already an improvement over a previously reported representative route via FDCA (0.22)[6,18] (see calculation details in Table S6), where the higher E-factor for the latter route is caused mainly by the low selectivity in the challenging hydrogenation of FDCA to THFDCA.

Further investigations focused on exploring less severe conditions. At lower temperature (90 °C) and a shorter reaction time, Au/HT-1 still exhibited a good activity (conv. > 72%, Table 1, entry 5), whereas Au/HT-2 and Au/HT-3 showed almost no significant activity (conv. < 20% and <5% yield of combined oxidized products, Table 1, entries 6−7). When the reaction temperature was further decreased to 70 °C, Au/HT-1 also showed no significant activity (Table 1, entry 8). The batch reproducibility was investigated using

DOI: 10.1021/acssuschemeng.8b03821
ACS Sustainable Chem. Eng. 2019, 7, 4647−4656

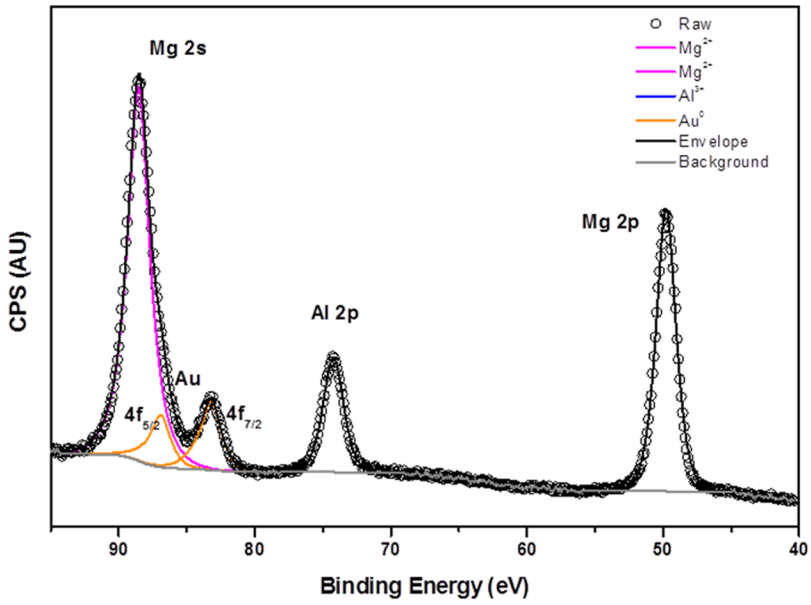

Figure 2. XPS data for full region of fresh Au/HT-1 catalyst. Au 4f and Mg 2s peaks were deconvoluted by constraining the Mg 2s peak position, area, and fwhm to the Mg 2p peak. The black lines represent the overall fit of the data.

Scheme 2. Oxidation Routes Using Au/HT Catalysts for (a) THFDM to THFDCA and (b) HMF to FDCA

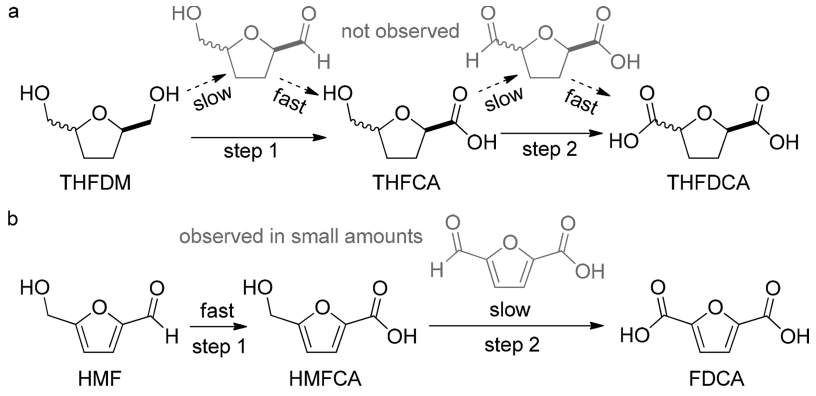

separately synthesized batches of the Au/HT-1 at 90 °C and 5 h reaction time (Table 1, entry 5). These experiments showed a maximum error in substrate conversion and product formation of 10 mol %, which could be due to experimental fluctuations between the heating profiles for different batches that arose from the use of different reactor set-ups.

TEM images showed particle size distributions from 0.5 to 4.5 nm (Figure 1) confirming the synthesis of nanoparticles on the all HT supports, which are smaller compared to those earlier reported for ammonia precipitation on HT support[18] but comparable to those obtained from urea precipitation on titania.[30] X-ray photoelectron spectroscopy (XPS, Figure 2) indicated that all gold is in the metallic Au^0 oxidation state with a binding energy of 83.2 eV (Table S4 and Figure S10). This is below the range of bulk Au^0 with a typical Au $4f_{7/2}$ binding energy between 87.9 and 84.2 eV. However, in the case of more spherical Au particles, the binding energies can be lowered down to 83.0 eV.[36,37] The high activity of all Au/HT catalysts at 110 °C can be related to the average small gold particle size. On the other hand, at the lower temperature, the high Mg/Al ratio (4.1, which decreased to 3.7 after metal loading, Tables S1 and S2) and low basicity of the HT-1 support (Table S1) can lead to increased activity. Basic sites derived from hydroxyl groups and Mg−O pairs can activate the aldehyde intermediate toward formation of the corresponding carboxylic acid. Similarly, Wang et al. showed that a Mg/Al ratio close to 4.9 had a positive effect on HMF oxidation in experiments using HT with different Mg/Al ratios loaded with Pd nanoparticles.[24] Au/HT-2 and Au-HT-3 might suffer from rate limitation related to ineffective product desorption due to the higher number of basic sites of the supports (Table S1).

Reaction Pathways and Possible Mechanism. The main intermediate product (THFCA) was successfully isolated and characterized by ^{1}H NMR and ^{13}C NMR spectroscopy (structure in Scheme 2a and NMR data in Figures S2 and S3). In our experiments, no aldehyde intermediates were identified, although some unidentified minor products could be observed in our HPLC profiles (Figure S4). The observation of THFCA as a major intermediate demonstrates that the oxidation sequence does not proceed through the diformyl intermediate as is observed for the oxidation of HMF with some oxidation systems.[18−20,24,35,38−45] In our experiments, the hydroxyl group of THFDM is first oxidized to the aldehyde group, which is readily transformed into the carboxylic acid in both the first and the second step of the oxidation sequence (Scheme 2a). This reaction pathway from THFDM toward THFDCA is

DOI: 10.1021/acssuschemeng.8b03821
ACS Sustainable Chem. Eng. 2019, 7, 4647−4656

consistent with the oxidation mechanism of HMF to FDCA presented by Gupta et al.,[18] over similar Au/HT catalysts, but prepared using a different reducing agent yielding larger Au particles, which proceeds through the monoacid intermediate 5-hydroxymethyl-2-furancarboxylic acid (HMFCA) and thus also shows relatively faster oxidation of the aldehyde compared to the alcohol (Scheme 2b). However, the 49% yield of THFDCA at 89% conversion using Au/HT-1 (Table 1, entry 4) differs significantly from HMF oxidation,[35] for which a threshold conversion >80% of HMF to HMFCA (step 1) was reported to be required before effective oxidation of HMFCA to FDCA was observed (step 2). On the other hand, it was shown that when using HMFCA as the starting substrate, the formation of FDCA was not limited by substrate or intermediate inhibition. It was concluded that high concentrations of HMFCA from the first oxidation step compared to the substrate (HMF) are needed to compete effectively with the relatively stronger adsorbed aldehydes on the catalyst. This limitation can be avoided by protection of the aldehyde group of HMF using a diol to give improved FDCA yields.[39] The contrast to our results arises from the different non-aldehyde-containing starting material (THFDM). Because the oxidation of aldehydes is relatively fast, no buildup of the aldehyde intermediates is observed. This limits the effect of competitive adsorption between the substrate and these intermediates in these batch experiments.

Catalyst Stability. A spent Au/HT-1 catalyst, originally obtained from a scale-up synthesis, was reused after extensive washing and drying at 90 °C in batch reactors (Figure 3,

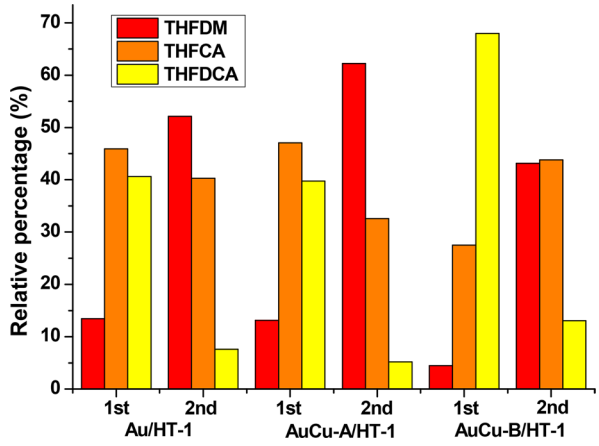

Figure 3. Recycle study of catalysts for THFDM oxidation. Reaction conditions: 30 mL of 0.02 M THFDM aqueous solution, THFDM/Au = 40:1 (molar ratio), catalyst amount ca. 0.17 g, 30 bar air pressure, 600 rpm, 5 h, 90 °C.

columns 1 and 2). Disappointingly, this showed that the activity of the catalyst dropped drastically after one use. Chemical analysis (ICP) of Au/HT-1 revealed no leaching of Au (Table S4). XPS results (Figure 4, right; Figure S5 for full region) indicated gold is still in the metallic Au^0 oxidation state. Figure 4 also shows the gold nanoparticles of the spent Au/HT-1 catalyst (left) after reaction by TEM analysis. The mean particle size of Au/HT-1 increased from 2.2 to 9.1 nm after one run. The agglomeration of gold nanoparticles is the most likely reason for the observed deactivation of these catalysts. In terms of the stability of the support, 5.4 wt % loss of the magnesium from the support was observed (Table S4). To exclude the hypothesis of leached support acting as a homogeneous base, we also performed a reaction with the same amount of $MgCl_2$ as was observed to be lost from the catalyst. In this experiment, no THFDM conversion was observed (Table S5, entry 1). Additionally, we physically mixed a HT support with another supported gold catalyst (Au/TiO_2), which gave no improved reactivity compared to (Au/TiO_2) by itself (17% after 5 h at 110 °C, Table S5 entries 2 and 3). Based on above results, we believe that a synergistic effect between the gold nanoparticles and the HT support results in the observed activity and selectivity in these reactions. Interestingly, Au/TiO_2 mixed with another $Ba(OH)_2$ as external base did show improved catalyst activity (97% conversion, 89% THFDCA, Table S5, entry 4).

The Influence of the Addition of Copper. As the potential for reuse of the monogold catalysts was limited, bimetallic catalysts were targeted next. The oxidation activity, selectivity, and stability of gold catalysts can be modified by alloying Au with another metal such as Pd,[40,46] Pt,[47] and Cu.[48] Recently, Pasini et al.[49] showed that bimetallic gold−copper catalysts display superior activity compared to monometallic gold catalysts in the oxidation of HMF. Due to copper being an abundant element and thus the most sustainable option, CuAu nanoparticles supported on HT-1 were prepared by sequential deposition−precipitation. Two different gold−copper bimetallic catalysts were prepared, by calcination either in air (AuCu-A/HT-1) or in H_2 (AuCu-B/HT-1) at 200 °C. XPS analysis showed that the gold was exclusively in the metallic state, matching with literature data on similar catalysts,[30] while copper was present also in higher oxidation states (Figure S11). Additionally, the gold exhibited higher binding energy (83.5 eV for AuCu-A/HT-1 and 83.4 eV for AuCu-B/HT-1) compared to that in the monometallic samples (83.2 eV for Au/HT-1) suggesting less spherical gold particles in the Au−Cu catalysts (Table S4 and Figure S11).[36,37] TEM analysis of the prepared bimetallic catalysts showed particle sizes of 0.9 and 1.0 nm for AuCu-A/HT-1 and AuCu-B/HT-1 respectively (Figure S6a,b). These were smaller compared to the 2.2 nm particle size obtained for the monometallic Au/HT-1. The small particle size and low loading of these particles meant that no signals for these metals were observed in XRD (Figure S1), and TEM-EDX was not successful due to the low metal loading and particle size.

Next, these catalysts as well as a separately prepared CuO/HT-1 catalyst were applied in the oxidation THFDM at 90 °C. No conversion was found for the CuO/HT-1 catalyst (Table 2, entry 1), which proved that gold is required for the oxidation of THFDM under these conditions. AuCu-A/HT-1 showed somewhat lower conversion of THFDM compared to Au/HT-1, whereas AuCu-B/HT-1 showed similar THFDM conversion (Table 2, entries 2 and 3, compared to Table 1, entry 5). Both bimetallic catalysts were slightly less selective to THFCA and THFDCA compared to the monometallic Au/HT-1 catalyst. No other intermediates could be identified from the solution, although buildup of other oxidation intermediates on the surface could not be excluded. Overall, no significant improvement was found in the reaction at 90 °C compared to Au/HT-1. However, when the reactions were performed at 70 °C, the bimetallic catalysts showed significant oxidation activity, while the monometallic catalysts did not (Table 2, entries 4 and 5, compared to Table 1, entry 8). An explanation for the increased activity of AuCu bimetallic catalysts at lower temperature is that the Cu in the form of CuO contains an

DOI: 10.1021/acssuschemeng.8b03821
ACS Sustainable Chem. Eng. 2019, 7, 4647−4656

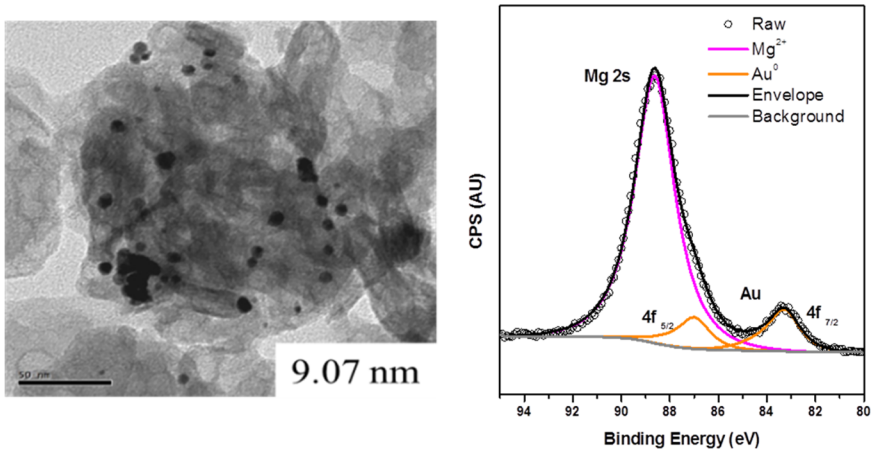

Figure 4. TEM image (left) and XPS data (right) of the spent Au/HT-1 catalysts with average particle size in the lower right corner (Figure S8 for distribution). Au 4f and Mg 2s peaks were deconvoluted by constraining the Mg 2s peak position, area, and fwhm to the Mg 2p peak. The black lines represent the overall fit of the data.

Table 2. Experimental Results for the Oxidation of THFDM Using Au–Cu/HT Catalysts[a]

					yield (%)	
entry	catalyst	time (h)	temp (°C)	conv. (%)	THFCA	THFDCA
1	CuO/HT-1	5	90	0	0	0
2	AuCu-A/HT-1	5	90	52	25	17
3	AuCu-B/HT-1	5	90	73	36	28
4	AuCu-A/HT-1	5	70	20	18	2
5	AuCu-B/HT-1	5	70	19	17	2
6	AuCu-A/HT-1	24	70	66	38	11
7	AuCu-B/HT-1	24	70	47	24	4

[a]Reaction conditions: 30 mL of 0.02 M THFDM in water, THFDM/Au = 40:1 (molar ratio), catalyst amount ca. 0.17 g, 30 bar air pressure, 600 rpm.

oxygen atom that is basic enough to abstract the proton from the hydroxyl group and thus act in synergy with the hydride abstraction by Au.[50] Unfortunately, TEM images of the bimetallic catalysts after 24 h reaction (Table 2, entries 6 and 7) also showed particle agglomeration (Figure S6c,d). The mean particle sizes of AuCu-A/HT-1 and AuCu-B/HT-1 increased from 0.9 and 1.1 nm to 3 and 3.6 nm, respectively. This indicates increased stability compared to the monometallic Au catalysts, which could be related to the observed less spherical shape of the gold nanoparticles, which is known to lead to higher stability.[36,37] In these experiments, AuCu-A/HT-1 showed overall higher activity as well as a smaller particle size increase, which could indicate that even though the initial activity is lower this catalyst has better long-term stability.

The reuse of spent AuCu-A/HT-1 and AuCu-B/HT-1 catalysts (now prepared from a 20 g scaled-up catalyst preparation) after extensive washing and drying was conducted at 90 °C in batch reactors (Figure 3, column 3–6). Also for these catalysts, the activities significantly decreased in the second run, which is in line with the observed particle size increase.

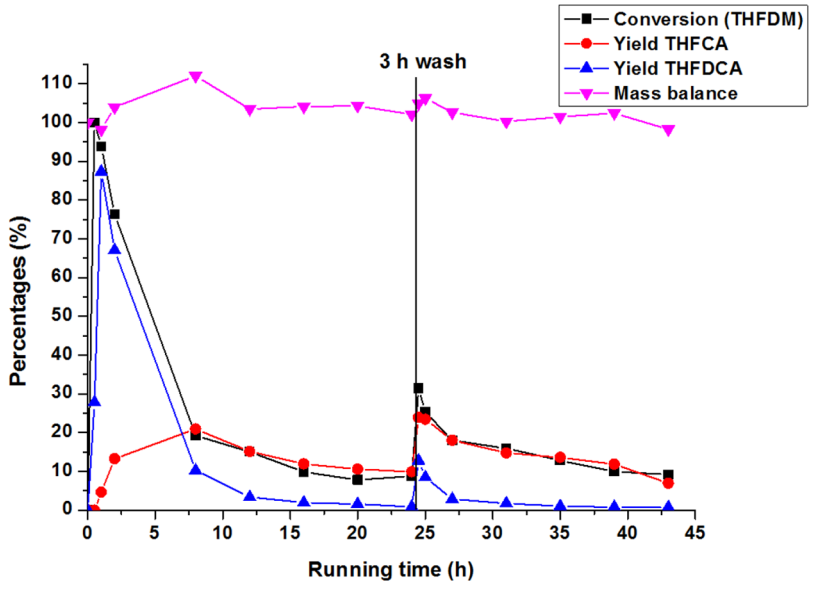

Figure 5. Results of AuCu-A/HT-1 catalyst in a continuous setup. Reaction conditions: flow 1.25 mL/min, 0.01 M THFDM aqueous solution with dipropyl sulfone as internal standard, 101 °C, 30 bar air pressure.

DOI: 10.1021/acssuschemeng.8b03821
ACS Sustainable Chem. Eng. 2019, 7, 4647–4656

THFDM Oxidation in a Continuous Setup. Catalyst activity and stability were further investigated using a continuous setup in which the product formation can be monitored over time (the setup is schematically depicted in Figure S7). Based on the results from 24 h batch reactions, AuCu-A/HT-1 was chosen to investigate the catalyst performance in time as this catalysts showed the lowest particle size increase and was thus suspected to suffer the least from catalyst deactivation. Figure 5 shows that at the start of the reaction full conversion of THFDM was achieved as well as high yield of THFDCA (up to 88%). Nevertheless, The catalyst deactivated rapidly over the first 5 h but reached a relatively steady state after 20 h at which the catalyst showed 10−15% THFDM conversion and mainly THFCA as oxidation product. After 24 h, a wash was performed only using water while maintaining the reaction temperature to see if the intermediate or end-product adsorption on the catalyst could be a cause for deactivation. Although the activity was not fully restored, which was in line with the recycling experiment performed in batch, the conversion activity for THFDM to THFCA and THFDCA was partially recovered showing around 40% conversion of THFDM and around 15% and 25% yield of THFDCA and THFCA, respectively. The overall deactivation in time is in line with the catalyst recycle studies in batch and is likely mainly due to particle agglomeration. However, the fact that washing the catalyst with water partly recovered catalyst activity indicated that poisoning by product adsorption can also be affecting the reaction. This was confirmed in a continuous reaction in which a crude oxidation mixture was collected, containing substrate and a mix of all intermediates and products and fed over a fresh catalyst bed resulting in no significant conversion. After washing the catalyst bed, the catalyst showed a conversion of 8% when a fresh THFDM stock was applied. This indicated that the deactivation of the catalysts can be related to the strong adsorption of oxidation intermediates or end products on the catalyst. Extrapolating data from early work on HMF oxidation, it is likely that aldehyde intermediates are the culprits causing catalyst deactivation by strong adsorption on the catalyst surface.[51] An experiment with a longer run time showed that the catalyst appears to reach a steady state (Figure S12). Here THFCA yield remains stable at about 10% even after 50 h.

CONCLUSION

Overall, this work demonstrates a new green route to access THFDCA and THFCA from HMF, which is achieved via a sequential catalytic reduction of HMF to THFDM followed by catalytic oxidation providing an overall yield of over 85% after two steps. This route can overcome selectivity problems that occur upon HMF oxidation to FDCA, as illustrated by a slightly beneficial overall E-factor. Gold-based catalysts supported on hydrotalcite provide an efficient catalytic system to oxidize THFDM to THFDCA with a high yield in a batch setup under relatively mild reaction conditions (91% yield, 30 bar air, 110 °C, 7 h). Smaller gold nanoparticle size and a lower number of basic sites of the HT support seem to positively influence the activity of the catalyst. Bimetallic gold copper catalysts were active at lower temperatures (70 °C). Both the monometallic and the bimetallic catalytic systems suffer from deactivation, which is mainly due to particle agglomeration and further affected by poisoning by oxidized intermediates. Additionally, some leaching of the support material was observed. Future work will focus on designing more stable catalysts for this reaction in order to increase the viability of the production of THFCA and THFDCA via this route, thus leading to further utilization of these compounds in renewable chemical product applications.

ASSOCIATED CONTENT

Supporting Information

The Supporting Information is available free of charge on the ACS Publications website at DOI: 10.1021/acssuschemeng.8b03821.

Physicochemical parameters, XRD patterns, different batch results, ^{13}C NMR, ^{1}NMR, XPS and ICP results, HPLC chromatogram, schematic representation of continuous setup, TEM images and particle size distribution (PDF)

AUTHOR INFORMATION

Corresponding Author

*P.J.D. E-mail: p.j.deuss@rug.nl.

ORCID

Emiel J. M. Hensen: 0000-0002-9754-2417
Paolo P. Pescarmona: 0000-0003-3608-6400
Hero J. Heeres: 0000-0002-1249-543X
Peter J. Deuss: 0000-0002-2254-2500

Author Contributions

Q.Y. and K.H. performed the experimental work under the scientific supervision of H.J.H., P.J.D., and P.P.P. Q.Y. and P.J.D. wrote the manuscript based on the master thesis written by K.H. and with input from the other authors. T.G.M. supervised the initial experimental work and contributed to design of the experiments at this stage together with I.C. S.v.d.V. from Kisuma synthesized the hydrotalcite supports. Z.T. and Q.Y. ran the TEM analysis. L.R. performed the ICP measurements. W.V., T.V., and E.J.M.H. performed and interpreted the XPS characterization.

Notes

The authors declare no competing financial interest.

ACKNOWLEDGMENTS

QY. acknowledges financial support from the China Scholarship Council (CSC). T.G.M. acknowledges financial support from Avebe and SNN ("Transitie II, Pieken in de delta"). The authors acknowledge Kisuma Chemicals for providing the hydrotalcite supports as well as Erwin Wilbers, Marcel de Vries, Anne Appeldoorn, Henk van de Bovenkamp, and Jan Henk Marsman for their analytical and technical support.

REFERENCES

(1) Bozell, J. J.; Petersen, G. R. Technology development for the production of biobased products from biorefinery carbohydrates—the US Department of Energy's "Top 10" revisited. *Green Chem.* **2010**, *12*, 539−554.

(2) van Putten, R.; van der Waal, J. C.; de Jong, E.; Rasrendra, C. B.; Heeres, H. J.; de Vries, J. G. Hydroxymethylfurfural, a versatile platform chemical made from renewable resources. *Chem. Rev.* **2013**, *113*, 1499−1597.

(3) Saha, B.; Abu-Omar, M. M. Advances in 5-hydroxymethylfurfural production from biomass in biphasic solvents. *Green Chem.* **2014**, *16*, 24−38.

(4) Taarning, E.; Nielsen, I. S.; Egeblad, K.; Madsen, R.; Christensen, C. H. Chemicals from renewables: aerobic oxidation of

DOI: 10.1021/acssuschemeng.8b03821
ACS Sustainable Chem. Eng. 2019, 7, 4647−4656

furfural and hydroxymethylfurfural over gold catalysts. *ChemSusChem* **2008**, *1*, 75−78.
(5) Bottari, G.; Kumalaputri, A. J.; Krawczyk, K. K.; Feringa, B. L.; Heeres, H. J.; Barta, K. Copper-zinc alloy nanopowder: a robust precious-metal-free catalyst for the conversion of 5-hydroxymethylfurfural. *ChemSusChem* **2015**, *8*, 1323−1327.
(6) Moore, J. A.; Kelly, J. E. An improved hydrogenation for the preparation of tetrahydrofurancis-2, 5-dicarboxylic acid. *Org. Prep. Proced. Int.* **1972**, *4*, 289−292.
(7) Tuteja, J.; Choudhary, H.; Nishimura, S.; Ebitani, K. Direct synthesis of 1,6-hexanediol from HMF over a heterogeneous Pd/ZrP catalyst using formic acid as hydrogen source. *ChemSusChem* **2014**, *7*, 96−100.
(8) Buntara, T.; Noel, S.; Phua, P. H.; Melian-Cabrera, I.; de Vries, J. G.; Heeres, H. J. Caprolactam from renewable resources: catalytic conversion of 5-hydroxymethylfurfural into caprolactone. *Angew. Chem., Int. Ed.* **2011**, *50*, 7083−7087.
(9) Kumalaputri, A. J.; Randolph, C.; Otten, E.; Heeres, H. J.; Deuss, P. J. Lewis acid catalyzed conversion of 5-hydroxymethylfurfural to 1,2,4-benzenetriol, an overlooked biobased compound. *ACS Sustainable Chem. Eng.* **2018**, *6*, 3419−3425.
(10) Isikgor, F. H.; Becer, C. R. Lignocellulosic biomass: a sustainable platform for the production of bio-based chemicals and polymers. *Polym. Chem.* **2015**, *6*, 4497−4559.
(11) Persson, P.; Sorensen, K.; Lundmark, S. Alkyd resin. WO Patent, WO2012/005645A1, 2012.
(12) Boussie, T. R.; Dias, E. L.; Fresco, Z. M.; Murphy, V. J. Production of adipic acid and derivatives from carbohydrate-containing materials. US Patent, US2010/0317822A1, 2010.
(13) Haworth, W. N.; Jones, W. G. M.; Wiggins, L. F. 1. The conversion of sucrose into furan compounds. part II. some 2:5-disubstituted tetrahydrofurans and their products of ring scission. *J. Chem. Soc.* **1945**, 1−4.
(14) Gilkey, M. J.; Mironenko, A. V.; Vlachos, D. G.; Xu, B. Adipic acid production via metal-free selective hydrogenolysis of biomass-derived tetrahydrofuran-2,5-dicarboxylic acid. *ACS Catal.* **2017**, *7*, 6619−6634.
(15) Pfeiffer, M.; Breitscheidel, B.; Grimm, A.; Morgenstern, H. Plasticizer composition containing polymeric dicarboxylic acid esters and 1,2-cyclohexane dicarboxylic acid esters. WO Patent, WO2017/055429A1, 2017.
(16) Gerk, P. M.; Walsh, S. W.; Wang, M.; Landsberg, A. K. Prodrugs utilizing a transporter-directed uptake mechanism. WO Patent, WO2012/048204A2, 2012.
(17) Gorbanev, Y. Y.; Kegnaes, S.; Riisager, A. Effect of support in heterogeneous ruthenium catalysts used for the selective aerobic oxidation of HMF in water. *Top. Catal.* **2011**, *54*, 1318−1324.
(18) Gupta, N. K.; Nishimura, S.; Takagaki, A.; Ebitani, K. Hydrotalcite-supported gold-nanoparticle-catalyzed highly efficient base-free aqueous oxidation of 5-hydroxymethylfurfural into 2,5-furandicarboxylic acid under atmospheric oxygen pressure. *Green Chem.* **2011**, *13*, 824−827.
(19) Mishra, D. K.; Lee, H. J.; Kim, J.; Lee, H. S.; Cho, J. K.; Suh, Y. W.; Yi, Y.; Kim, Y. J. $MnCo_2O_4$ spinel supported ruthenium catalyst for air-oxidation of HMF to FDCA under aqueous phase and base-free conditions. *Green Chem.* **2017**, *19*, 1619−1623.
(20) Dijkman, W. P.; Binda, C.; Fraaije, M. W.; Mattevi, A. Structure-based enzyme tailoring of 5-hydroxymethylfurfural oxidase. *ACS Catal.* **2015**, *5*, 1833−1839.
(21) Mobley, J. K.; Crocker, M. Catalytic oxidation of alcohols to carbonyl compounds over hydrotalcite and hydrotalcite-supported catalysts. *RSC Adv.* **2015**, *5*, 65780−65797.
(22) Davis, S. E.; Ide, M. S.; Davis, R. J. Selective oxidation of alcohols and aldehydes over supported metal nanoparticles. *Green Chem.* **2013**, *15*, 17−45.
(23) Gorbanev, Y. Y.; Kegnaes, S.; Riisager, A. Selective aerobic oxidation of 5-hydroxymethylfurfural in water over solid ruthenium hydroxide catalysts with magnesium-based supports. *Catal. Lett.* **2011**, *141*, 1752−1760.
(24) Wang, Y.; Yu, K.; Lei, D.; Si, W.; Feng, Y.; Lou, L.−L.; Liu, S. Basicity-tuned hydrotalcite-supported Pd catalysts for aerobic oxidation of 5-hydroxymethyl-2-furfural under mild conditions. *ACS Sustainable Chem. Eng.* **2016**, *4*, 4752−4761.
(25) Tsunoyama, H.; Sakurai, H.; Negishi, Y.; Tsukuda, T. Size-specific catalytic activity of polymer-stabilized gold nanoclusters for aerobic alcohol oxidation in water. *J. Am. Chem. Soc.* **2005**, *127*, 9374−9375.
(26) Fang, W.; Zhang, Q.; Chen, J.; Deng, W.; Wang, Y. Gold nanoparticles on hydrotalcites as efficient catalysts for oxidant-free dehydrogenation of alcohols. *Chem. Commun.* **2010**, *46*, 1547−1549.
(27) Wang, L.; Zhang, J.; Meng, X.; Zheng, D.; Xiao, F.-S. Superior catalytic properties in aerobic oxidation of alcohols over Au nanoparticles supported on layered double hydroxide. *Catal. Today* **2011**, *175*, 404−410.
(28) Zope, B. N.; Hibbitts, D. D.; Neurock, M.; Davis, R. J. Reactivity of the gold/water interface during selective oxidation catalysis. *Science* **2010**, *330*, 74−78.
(29) Davis, S. E.; Zope, B. N.; Davis, R. J. On the mechanism of selective oxidation of 5-hydroxymethylfurfural to 2,5-furandicarboxylic acid over supported Pt and Au catalysts. *Green Chem.* **2012**, *14*, 143−147.
(30) Sandoval, A.; Louis, C.; Zanella, R. Improved activity and stability in CO oxidation of bimetallic Au−Cu/TiO_2 catalysts prepared by deposition−precipitation with urea. *Appl. Catal., B* **2013**, *140*−*141*, 363−377.
(31) Pérez-Ramírez, J.; Abelló, S.; van der Pers, N. M. Memory effect of active Mg-Al hydrotalcite: in situ XRD studies during decomposition and gas-phase reconstruction. *Chem. - Eur. J.* **2007**, *13*, 870−878.
(32) Roelofs, J. C. A. A.; van Bokhoven, J. A.; van Dillen, A. J.; Geus, J. W.; de Jong, K. P. The thermal decomposition of Mg − Al hydrotalcites: effects of interlayer anions and characteristics of the final structure. *Chem. - Eur. J.* **2002**, *8*, 5571−5579.
(33) Tichit, D.; Bennani, M. N.; Figueras, F.; Ruiz, J. R. Decomposition process and characterization of the surface basicity of Cl^- and CO_3^{2-} hydrotalcites. *Langmuir* **1998**, *14*, 2086−2091.
(34) Ballarin, B.; Mignani, A.; Scavetta, E.; Giorgetti, M.; Tonelli, D.; Boanini, E.; Mousty, C.; Prevot, V. Synthesis route to supported gold nanoparticle layered double hydroxides as efficient catalysts in the electrooxidation of methanol. *Langmuir* **2012**, *28*, 15065−15074.
(35) Ardemani, L.; Cibin, G.; Dent, A. J.; Isaacs, M. A.; Kyriakou, G.; Lee, A. F.; Parlett, C. M. A.; Parry, S. A.; Wilson, K. Solid base catalysed 5-HMF oxidation to 2,5-FDCA over Au/hydrotalcites: fact or fiction? *Chem. Sci.* **2015**, *6*, 4940−4945.
(36) Schimpf, S.; Lucas, M.; Mohr, C.; Rodemerck, U.; Brückner, A.; Radnik, J.; Hofmeister, H.; Claus, P. Supported gold nanoparticles: in-depth catalyst characterization and application in hydrogenation and oxidation reactions. *Catal. Today* **2002**, *72*, 63−78.
(37) Radnik, J.; Mohr, C.; Claus, P. On the origin of binding energy shifts of core levels of supported gold nanoparticles and dependence of pretreatment and material synthesis. *Phys. Chem. Chem. Phys.* **2003**, *5*, 172−177.
(38) Ait Rass, H.; Essayem, N.; Besson, M. Selective aqueous phase oxidation of 5-hydroxymethylfurfural to 2,5-furandicarboxylic acid over Pt/C catalysts: influence of the base and effect of bismuth promotion. *Green Chem.* **2013**, *15*, 2240−2251.
(39) Kim, M.; Su, Y.; Fukuoka, A.; Hensen, E. J. M.; Nakajima, N. Aerboic oxidation of 5-(hydroxymethyl)furfural cyclic acetal enables selective furan-2,5-dicarboxylic acid formation with CeO_2-supported gold catalyst. *Angew. Chem., Int. Ed.* **2018**, *57*, 8235−8239.
(40) Wan, X. Y.; Zhou, C. M.; Chen, J. S.; Deng, W. P.; Zhang, Q. H.; Yang, Y. H.; Wang, Y. Base-free aerobic oxidation of 5-hydroxymethyl-furfural to 2,5-furandicarboxylic acid in water catalyzed by functionalized carbon nanotube-supported Au-Pd alloy nanoparticles. *ACS Catal.* **2014**, *4*, 2175−2185.
(41) Siyo, B.; Schneider, M.; Radnik, J.; Pohl, M.; Langer, P.; Steinfeldt, N. Influence of support on the aerobic oxidation of HMF

DOI: 10.1021/acssuschemeng.8b03821
ACS Sustainable Chem. Eng. 2019, 7, 4647−4656

into FDCA over preformed Pd nanoparticle based materials. *Appl. Catal., A* **2014**, *478*, 107−116.
(42) Neatu, F.; Marin, R. S.; Florea, M.; Petrea, N.; Pavel, O. D.; Parvulescu, V. I. Selective oxidation of 5-hydroxymethyl furfural over non-precious metal heterogeneous catalysts. *Appl. Catal., B* **2016**, *180*, 751−757.
(43) Artz, J.; Palkovits, R. Base-free aqueous-phase oxidation of 5-hydroxymethylfurfural over ruthenium catalysts supported on covalent triazine frameworks. *ChemSusChem* **2015**, *8*, 3832−3838.
(44) Han, X.; Geng, L.; Guo, Y.; Jia, R.; Liu, X.; Zhang, Y.; Wang, Y. Base-free aerobic oxidation of 5-hydroxymethylfurfural to 2,5-furandicarboxylic acid over a Pt/C−O−Mg catalyst. *Green Chem.* **2016**, *18*, 1597−1604.
(45) Siankevich, S.; Savoglidis, G.; Fei, Z.; Laurenczy, G.; Alexander, D. T. L.; Yan, N.; Dyson, P. J. A novel platinum nanocatalyst for the oxidation of 5-Hydroxymethylfurfural into 2,5-Furandicarboxylic acid under mild conditions. *J. Catal.* **2014**, *315*, 67−74.
(46) Gao, Z.; Xie, R.; Fan, G.; Yang, L.; Li, F. Highly efficient and stable bimetallic AuPd over La-doped Ca−Mg−Al layered double hydroxide for base-free aerobic oxidation of 5-hydroxymethylfurfural in water. *ACS Sustainable Chem. Eng.* **2017**, *5*, 5852−5861.
(47) Tongsakul, D.; Nishimura, S.; Ebitani, K. Platinum/gold alloy nanoparticles-supported hydrotalcite catalyst for selective aerobic oxidation of polyols in base-free aqueous solution at room temperature. *ACS Catal.* **2013**, *3*, 2199−2207.
(48) Sugano, Y.; Shiraishi, Y.; Tsukamoto, D.; Ichikawa, S.; Tanaka, S.; Hirai, T. Supported Au-Cu bimetallic alloy nanoparticles: an aerobic oxidation catalyst with regenerable activity by visible-light irradiation. *Angew. Chem., Int. Ed.* **2013**, *52*, 5295−5299.
(49) Pasini, T.; Piccinini, M.; Blosi, M.; Bonelli, R.; Albonetti, S.; Dimitratos, N.; Lopez-Sanchez, J. A.; Sankar, M.; He, Q.; Kiely, C. J.; Hutchings, G. J.; Cavani, F. Selective oxidation of 5-hydroxymethyl-2-furfural using supported gold−copper nanoparticles. *Green Chem.* **2011**, *13*, 2091−2099.
(50) Zhao, G.; Hu, H.; Deng, M.; Ling, M.; Lu, Y. G. Au/Cu-fiber catalysts with enhanced low-termperature activity and heat transfer for the gas-phase oxidation of alcohols. *Green Chem.* **2011**, *13*, 55−58.
(51) Mitsudome, T.; Noujima, A.; Mizugaki, T.; Jitsukawa, K.; Kaneda, K. Supported gold nanoparticles as a reusable catalyst for synthesis of lactones from diols using molecular oxygen as an oxidant under mild conditions. *Green Chem.* **2009**, *11*, 793−797.

DOI: 10.1021/acssuschemeng.8b03821
ACS Sustainable Chem. Eng. 2019, 7, 4647−4656